Biguanide Mono- and Bimetallic Zinc Complexes for the Highly-Efficient Ring-Opening (Co)polymerization of Lactides

Benjamin Théron,[a†] Lukáš Vlk,[a‡] Tomáš Chlupatý,[‡*] Marie-José Penouilh,[†] Eliška Procházková,[‖] Raluca Malacea-Kabbara,[†] Pierre Le Gendre,[†*] Aleš Růžička[‡*]

†Institut de Chimie Moléculaire de l'Université de Bourgogne (ICMUB, UMR-CNRS 6302), Université de Bourgogne, France

‡Department of General and Inorganic Chemistry, Faculty of Chemical Technology, University of Pardubice, Studentská 573, Pardubice 532 10, Czech Republic

‖Institute of Organic Chemistry and Biochemistry, Czech Academy of Sciences, Flemingovo nám. 2, Prague 160 00, Czech Republic

KEYWORDS. biguanide; zinc; ROP; copolymer.

ABSTRACT: One of the most urgent social demands on polymer chemistry is the design of an inexpensive, efficient, robust and non-toxic catalyst for the preparation of biodegradable polymers with good control of its properties. The dissymmetric ditopic doubly-deprotonable biguanide proligand (substituted 4,6-dimethoxypyrimidin-2-yl-guanidine – **1**) with dynamic behavior forms monometallic as well as bimetallic complexes when reacted with one or two equivalents of Et_2Zn or $Zn[N(SiMe_3)_2]_2$. In the monometallic complexes **2** and **4**, zinc atoms primarily occupy a position within the six-membered ring. In the bimetallic complexes **3** and **5**, the adjacent ethylzinc- and zinc-amide moieties are coordinated in a bidentate fashion by the guanidinate-like part of the ligand. The ethylzinc complexes **2** and **3** are inactive in the ring-opening polymerization (ROP) of *rac*-lactide, whereas the performance of the zinc amides **4** and **5** activated by iPrOH is among the highest observed. In complex **5**, the positions of the two zinc ions can be interchanged, which could explain the ability of this "dissymmetric" bimetallic complex to promote the ROP of lactide (LA) at both Zn sites to form polylactide (PLA) chains with a unimodal molecular-weight distribution. One-pot preparation of various di- or oligoblock copolymers is possible by the consecutive living copolymerization of β-butyrolactone and *L*-, *D*- or *rac*-lactides, leading to the precise control of its microstructure.

Introduction

After a hundred years of continuous development, polymeric materials based on repeating units of main-group elements have found widespread practical application in both everyday life and industry. Conventional (*i.e.* petroleum-based non-biodegradable) plastics have transformed our society and are used in all aspects of our daily lives. However, their impact on the environment is considerable and no longer tolerable. Polylactide (PLA) is the most promising biobased and biodegradable alternative to petrochemical plastics.[1] It is now being successfully employed in various fields such as 3D printing, medical applications, food packaging, disposable tableware, textiles, agriculture and automotive.[2] A downside to this development is that the industrial production of PLA is mainly attached to the ring-opening polymerization (ROP) of lactide in the presence of tin octoate, whose impact on the environment remains questionable. Great efforts have been devoted to the development of tin-free catalysts. As metal complexes and organometallic species often suffer from the presence of toxic heavy or expensive noble metals and high specificity for a desired reaction or process, one possibility is the application of post-transition metals, specifically zinc and its complexes, which have already shown their potential in many organic transformations or as cheap, environmentally benign and sustainable alternatives to conventional transition-metal catalysts. Zinc catalysts provide some of the best performance in the ROP of lactides, notably in terms of activity. The pioneering works of Coates have shown that *β*-diketiminate (BDI) ligands associated with Zn(II) lead to highly efficient systems (Fig. 1).[3] More recently, Robinson has described exceptional activity at room temperature for the ROP of LA (TOF_{max} = 13'950 h^{-1}) using Zn complexes supported by a dissymmetric version of these BDI ligands (*N*-Aryl/*N*-alkyl).[4]

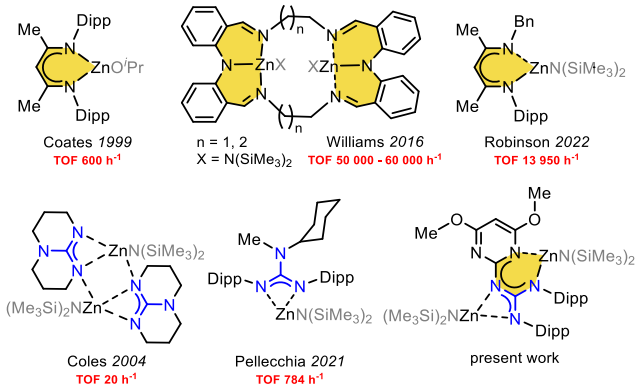

Figure 1. The most active BDI (ring highlighted in gold), BDI-like and guanidinate (in blue) zinc complexes in lactide ROP.

Remarkably, the highest TOF (60'000 h^{-1}), reported by Williams,[5] has been reached by a dizinc catalyst also coordinated by a "BDI-like" ligand, which can be classified as ditopic as well. Coles[6] and Pellechia[7] have demonstrated that highly π-electron-conjugated guanidinate ligands associated with zinc are also pertinent to the lactide ROP reaction. Recently, epoxide-promoted polymerization of lactides mediated by the low loading of the zinc-guanidine complex has been tested under industrial conditions.[8] In addition, during the completion of this work, Robinson reported on stereoblock polyesters *via* irreversible chain-transfer ring-opening

polymerization using a combination of the previously reported highly-active lactide polymerization process promoted by zinc BDI species[4] and the yttrium phenoxide co-initiated polymerization of *β*-butyro- or *β*-valerolactone, yielding stereoblock atactic-syndiotactic polyhydroxyalkanoates with good control of the composition, molecular weight and mechanical properties.[9] As summarized in the excellent review on strategies for preparation of stereoblock copolymers by Mehrkhodavandi[10], the most efficient catalytic systems are based on versatile indium[11-14] and magnesium[15] complexes or tin octoate[16]. It is worth noting that also zinc-based initiators allowed an excellent access to various oligo-block polyesters and carbonates. Kol[17], Pellecchia[18] and Phomphrai[19, 20] made their lactide homo- and copolymeric materials thanks to pyridylamido or phenoxyamido zinc initiators.

During the last 15 years, reports of block polyhydroxybutyrate-containing copolymers, which exhibit interesting material properties, were rather scarce. Rieger[21] used zinc β-diketiminate complexes as initiators of terpolymerization of β-butyrolactone, oxiranes and CO_2. Aluminum-based salen[22], phenoxyimine[23, 24] and phenolate[25] catalysts were also able to promote β-butyrolactone and lactide copolymerization with narrow polydispersities of the formed chains. Indium complex from the family of multi-talented [(NNO)In] chlorides or alcoholates[11-14], later shown to be active with low catalyst loadings[13], or under air atmosphere[14], albeit with reaction times of 16 hours. For the first time, a tri-block PLA-PHB-PLA was obtained in 2013[11] through sequential addition of the monomers. Other groups used yttrium[22, 26] hafnium[27] and copper[28] metals bearing mostly *N*- and *O*-donor ligands.

Based on these literature facts, we hypothesized that the biguanide derivative **1** (Figs. 1 & 2), mimicking both BDI and guanidinate moieties, with highly conjugated π-electron density and structural versatility, could be a suitable ligand to chelate one or two Zn atoms in a variable bonding fashion and (co)-initiate the ROP of lactides efficiently.

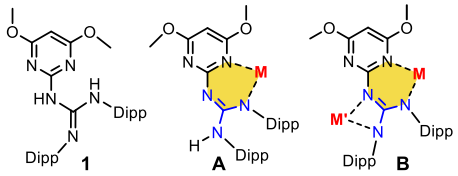

Figure 2. Possible monometallic A and bimetallic B complexes (among others) obtained from the biguanide proligand **1.**

Results and Discussion

The biguanide proligand **1** was prepared according to our previous paper from extremely cheap chemicals by one-pot high-yield synthesis (see SI)[29]. Thanks to the connection of a pyrimidin-2-amine moiety and a guanidine fragment, the structure of **1** resembles a part of such macrocyclic ligands as porphyrines, phthalocyanines and other biologically important species (guanine derivatives), but, more interestingly, also a substituted biguanide, which demonstrated biological activity and medicinal applications as well.[23-26] The structural versatility of highly π-electron conjugated **1** arises from the presence of three types of nitrogen atoms – two pyrimidine nitrogens, two secondary amines and one secondary imine – interconnected *via* two central carbon atoms (abbreviated as Ar_q^{Gua} and Ar_q^{Prm}) of the planar N_5C_2 skeleton. In **1**, this arrangement leads to the coexistence of different isomers and tautomers in equilibrium (Fig. 3). This equilibrium in solution is solvent- and temperature-dependent and can be easily monitored by NMR spectroscopy. In both non-polar (benzene) and polar (THF) solvents, two sets of signals (the ratios of 90:10 in THF and 95:5 in benzene at room temperature) were detected, indicating the presence of two different species. DFT calculations uncovered four possible forms. While two tautomers are energetically close to each other (**1A** and **1B**; less than 1 kcal/mol), another two possible forms with the ΔG of 4.3 and 7.8 kcal/mol are higher than the tautomer **1A**, indicating less than 1% population in the equilibrium (details in SI, page S9). For further investigation of these tautomeric equilibria, the experimental ^{13}C chemical shifts were correlated with the calculated chemical shielding constants. The correlations (Fig. S7 in SI) indicated that the major form in THF was the enamine tautomer **1A**, while the minor form was identified as the imine tautomer **1B**. The tautomer **1A** was also found in solid state by scXRD techniques (Fig. S9 in SI).

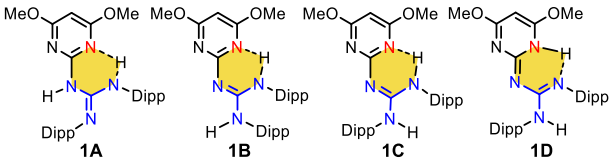

Figure 3. Possible tautomers/isomers of the proligand **1**.

Generally, such a dissymmetric biguanide structure can be seen as a potentially doubly-deprotonable proligand with the possibility of "aza-*β*-diketiminate" or guanidinate-chelate-ring formation. Surprisingly enough, structurally close but symmetric bis-guanidinate zinc hydride and ditopic conjugated bis-guanidine aluminum and lithium complexes able to chelate two metal atoms have very recently been used for the catalytic reduction of heteroallenes or carbonyl groups.[34-37]

To confirm or disprove our hypothesis, we prepared mono-/homobimetalic zinc biguanide complexes **2**–**5** in excellent isolated yields over 80% (Scheme 1). Particularly, the reaction of an equimolar amount of diethylzinc or zinc bis(hexamethyldisilazide) with the proligand **1** has afforded the isostructural complexes **2** and **4**.

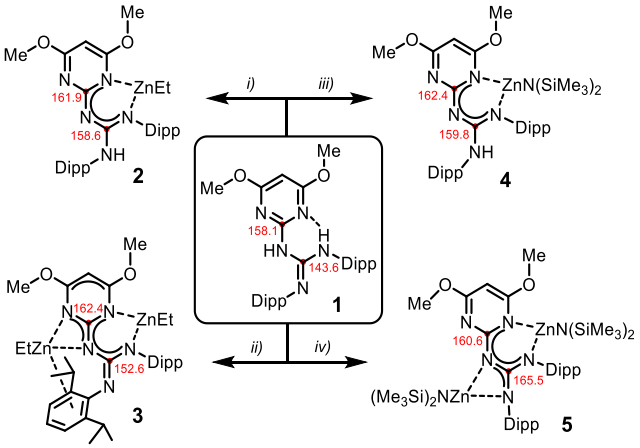

Scheme 1. The synthesis of the mono-/homobimetalic zinc biguanide complexes **2**–**5**: *i*) Et_2Zn, hexane, −80 °C to RT, 24 hours; *ii*) 2 Et_2Zn, Et_2O, −80 °C to RT, 7 hours; *iii*) $Zn[N(SiMe_3)_2]_2$, Et_2O, −80 °C to RT, 24 hours; *iv*) 2 $Zn[N(SiMe_3)_2]_2$, Et_2O, −80 °C to RT, 7 days. Significant ^{13}C NMR chemical shifts (δ of Ar_q^{Prm} and Ar_q^{Gua}) are highlighted in red and marked with red dots – for **5**, the values recorded at 373 K are presented.

Only one resonance for a hydrogen atom belonging to the NH group at 5.50 and 5.62 ppm in C_6D_6 has been detected in the ^1H NMR spectra of **2** and **4**, respectively (Fig. S54 and S70 in SI). These hydrogen atoms are undoubtedly connected to the nitrogen atoms of the Dipp groups as corroborated by 2D NMR techniques (^1H,^{13}C-HMBC, Fig. S57–S58 and S73–S74 in SI). The chemical-

shift values are up to 4 ppm upfield-shifted when compared to the same parameter found for the starting **1**. An obvious explanation arose from the fact the NH group is not connected by a hydrogen bridge to another part of the molecule. This arrangement is only possible when the zinc atom is coordinated to the six-membered ring. Unlike in **1**, there is no hydrogen atom on the central nitrogen (or N3 according to the crystallographic numbering – Fig. 4) in **2** and **4**, with this deprotonated nitrogen being a part of a highly conjugated π-electron system. The observed phenomenon is also reflected in the remarkable downfield shift (the Δδ of 15 ppm) of the Ar_q^{Gua} carbon atom in the ^{13}C NMR spectra of both **2** and **4** complexes measured in C_6D_6. On the other hand, all Ar_q^{Prm} carbon atoms resonate at a similar value (~162 ppm) (Scheme 1).

The solid-state behavior of the isostructural mononuclear complexes **2** and **4** shows that the zinc atoms are chelated by the N1 and N5 atoms of both pyrimidine and guanidine domains (Fig. 4), thus forming six-membered triazazincacycles, which are reminiscent of the zinc β-diketiminate complexes[38-41], phthalocyanines[42], or guanidinates and biguanides[37, 43]. In both complexes, the interatomic distances are almost the same. The N2 atom, bearing an acidic hydrogen, is excluded from the highly π-electron-conjugated planar system, as documented by C1–N2 distances (Fig. 4), which are the longest in the series, but still longer than in **1** (Fig. S9 in SI, 1.283(2) Å). The only difference in the molecular structures of **2** and **4** is caused by the more sterically demanding disilazide ligand in **4**, which displaces the zinc atom from the plane of the ligand by 0.588 Å. There is a head-to-tail (MeOCC(H)COMe with NCN) π-π stacking interaction of the neighboring pyrimidine rings (~ 3Å) in **2** and a head-to-head interaction of MeOCC(H)COMe groups (~ 3.5Å) in **4**.

The same synthetic approach (in Et_2O, −80 °C), in the molar ratio of 1:2, has also been used for the preparation of the homobimetalic zinc biguanides **3** and **5**. In the case of the synthesis of **3**, the reaction procedure is complex, and after the addition of diethylzinc, the reaction time must be limited to 7 hours only. When the product is kept in solution for a longer time, the subsequent decomposition of **3** to **2** (and some unidentified ethylzinc moiety) is observed. In order to maximize the yield, different reaction times and stoichiometry have been investigated (for more details, see SI, pp. S13–S29).

The structure of both complexes **3** and **5** was determined by NMR spectroscopy, where the spectral pattern of **3** was similar to that shown in **2** and **4**. However, the complex **5** behaved differently, as indicated by the significant NMR-signal broadening. In order to investigate fluxional behavior of **5**, variable-temperature NMR measurements were performed. Although distinct sets of the signals of peripheral methyl and methine groups (203 K in Tol-d_8; for VT NMR measurements, see SI, Fig. S23–S24) were recorded, the spectra exhibit only one set of signals for the biguanide carbon atoms of the core of the compound. In particular, for Ar_q^{Gua}/Ar_q^{Prm}, the resonances were found at 164.9/159.3 ppm (compare with 165.5/160.6ppm, recorded at 373 K, and with 152.6/162.4 ppm for **3**; see Scheme 1). This indicates that in **5**, the guanidinato group is more involved in the coordination of the second zinc atom than the pyrimidine group. In the ^1H NMR spectra, the hydrogen atom located on the top of the pyrimidine part of complex **5** (5.1 ppm at 295 K in C_6D_6) is similarly downfield-shifted to monometallic **2**, **4** and bimetallic **3**, but different by Δδ 0.4 ppm from the value found for the proligand **1**.

The solid-state structure of **3** shows the Zn1 atom chelated in the six-membered ring with a planar arrangement and Zn1–N5 distances only about 0.05 Å longer than in **2** (Fig. 4). The Zn2 atom is bound anisobidentately to the guanidinate group (Zn2–N3=1.9699(17) and Zn2–N4=2.3864(18)Å) with the N3–Zn2–N4 angle of 60.69(6)°. The adjacent contact of the Zn2 to the

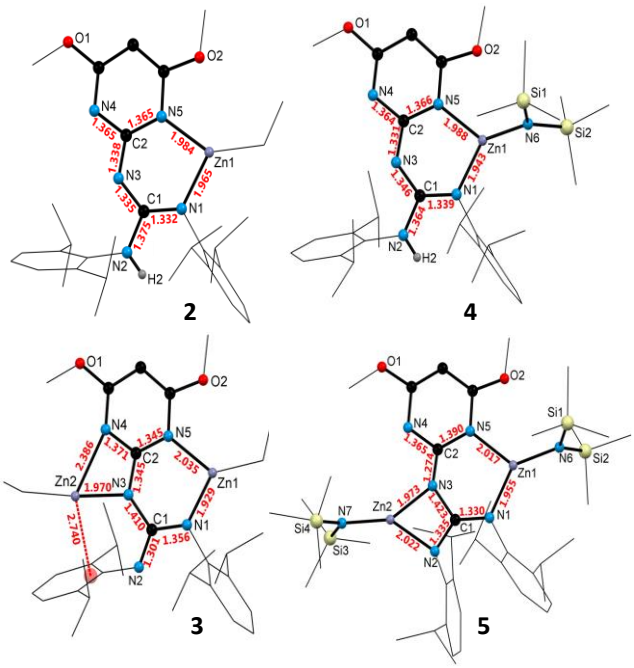

Figure 4. Molecular structures of **2**, **3**, **4** and **5**. Isopropyl, phenyl, ethyl and some of the methyl groups are shown as wireframes for clarity. Selected bond lengths (Å) and angles (°) (in red, without standard deviations) for 2: C2–N3–C1 126.93(16), N1–C1–N2 118.97(16); for 3: C2–N3–C1 126.91(10), N1–C1–N2 118.56(9); for 4: C2–N3–C1 127.7(3), N1–C1–N2 117.5(3); for 5: C2–N3–C1 131.4(12), N1–C1–N2 130.7(12). The full list of data is given in the SI (Fig. S25).

neighboring phenyl ring *via* η^3-fashion (2.602 Å) brings the zinc out of the planar environment of the ligand by 0.269 Å. The second compound, the dinuclear complex **5**, bearing one disilazide group on each zinc atom, has the ligand core and both zinc atoms nearly in plane, which is enabled by the elongation of the N1–N5 distance by ~0.1Å and the widening of the N2–C1–N3 angle by ~6°. The second change, together with the inversion of the position of the phenyl ring on the N2 atom, despite the high steric repulsion of both Dipp groups (the distance of ~3.5Å), has unblocked the possibility of coordinating the Zn2 atom to another guanidinate moiety in a nearly isobidentate fashion by N2 and N3 atoms (1.973(12) and 2.022(11)Å, angle 66.6(5)). This arrangement has caused non-negligible changes within the bonding of the ligand system, where the N2–C1, N3–C2 and C5–O2 bonds are significantly shortened and the N4–C3 one elongated by ~0.03–0.1Å when compared to the rest of the compounds (see SI – Fig. S25).

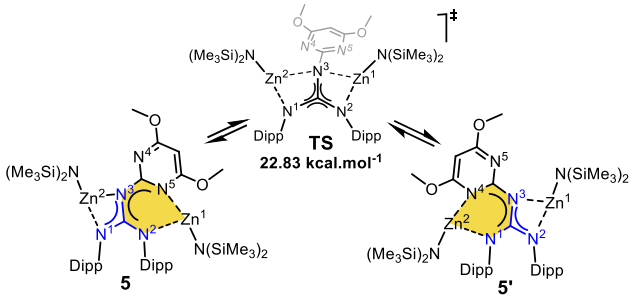

Figure 5. Simplified isomerization pathway of **5** leading to chemically identical species. Only lower energy TS is shown. A more detailed view is given in SI (Scheme S2).

Table 1. The ROP of *rac*-lactide mediated by the biguanide–Zn complexes **4** and **5** – selected experiments[a,b]

Entry	Cat.	[rac-LA]:[cat]$_0$:[^{i}PrOH]	time [min]	conv. [%]	$M_{n,\,theo}$[d] [g.mol^{-1}]	$M_{n,\,exp}$[f] [g.mol^{-1}]	Đ[f]	P_r[g]	TOF [h^{-1}]
1	**4**	100:1:0	2 h	61	8800[e]	188,000	1.11	n.d.	30
2	**5**	100:1:0	2 h	32	2300[e]	54,100	1.66	n.d.	8
3	**4**	100:1:1	1	98	14,100	13,400	1.07	0.63	5880
4	**5**	100:0.5:1	1	96	13,800	18,700	1.13	n.d.	5760
5	**5**	100:1:1	1	80	11,500	15,800	1.24	n.d.	2400
6	**4**	1000:1:1	5	94	135,000	116,200	1.08	n.d.	11,280
7	**4**	1000:1:1	3	83	119,600	110,700	1.08	0.65	16,600
8	**4**	5000:1:10	30	88	63,400	55,900	1.04	n.d.	8800
9	**5**	5000:0.5:10	20	90	64,900	67,100	1.04	n.d.	13,500

[a] All data can be found in SI – Table S2; polymerization conditions: [*rac*-LA]$_0$ = 1.5 M, CH_2Cl_2, 25°C. [b] Reactions performed with a batch of recrystallized and sublimed LA. [c] Monomer conversion. [d] Calculated using $M_{n,\,theo}$ = [*rac*-LA]$_0$/[^{i}PrOH]$_0$ × M_{LA} × conversion. [e] Calculated using $M_{n,\,theo}$ = [*rac*-LA]$_0$/[Zn]$_0$ × M_{LA} × conversion. [f] Measured by GPC in THF (45 °C) using PS standards and corrected by applying the appropriate correction factor (0.58). [g] Determined from the methine region of the HD ^{1}H NMR spectrum.

Table 2. The ROP of *β*-butyrolactone and *co*ROP with lactide mediated by the biguanide–Zn complexes **4** and **5**[a].

En-try	Cat.	[M_1]:[M_2]:[M_3]: [cat]$_0$:[^{i}PrOH]	M_1	M_2	M_3	T_1 [°C]	T_2 [°C]	T_3 [°C]	t_1 [min]	t_2	t_3 [min]	M_1 conv. [%][b]	M_2 conv. [%][b]	M_3 conv. [%][b]	$M_{n,\,theo}$[c] [g.mol^{-1}]	$M_{n,\,exp}$[d] [g.mol^{-1}]	Đ[d]
1	**4**	100:0:0:1:1	BL	-	-	45	-		180	-	-	94	-	-	8800	6200	1.04
2	**5**	100:0:0:0.5:1	BL	-	-	45	-		180	-	-	63	-	-	5400	5000	1.26
3	**4**	50:50:0:1:1	*L*-LA	BL	-	20	45		1	3 h	-	100	38	-	8800	7000	1.45
4	**4**	50:50:0:1:1	*L*-LA	BL	-	20	45		1	24 h	-	100	84	-	10,800	8300	1.64
5	**4**	50:50:0:1:1	BL	*L*-LA	-	45	20		180	1 min	-	90	90	-	10,400	11,000	1.06
6	**4**	50:50:50:1:1	BL	*L*-LA	D-LA	45	20	20	210	15 min	25	93	99	91	17,700	14,000[e]	-
7	**4**	50:50:50:1:1	*rac*-LA	BL	*rac*-LA	20	45	20	2	5 h[f]	30	99	95	85	17,300	13,200	1.26
8	**5**	50:50:50:0.5:1	*rac*-LA	BL	*rac*-LA	20	45	20	2	40 h	360	99	93	95	18,000	16,000	1.29

[a] Polymerization conditions: [M]$_0$ = 1.5 M, [**4**]$_0$ = 0.015 mM, CH_2Cl_2. [b] Monomer conversion. [c] Calculated using $M_{n,\,theo}$ = [*rac*-LA]$_0$/[^{i}PrOH]$_0$ × M_{LA} × $Conv._{LA}$ + [*rac*-BL]$_0$/[*i*PrOH]$_0$ × M_{BL} × $Conv._{BL}$. [d] Measured by GPC in THF (45°C) using PS standards and corrected by applying weighted correction factors (0.58 for PLA and 0.54 for PHB). [e] Determined by DOSY NMR. [f] Then left for 5 days.

To explain the dynamic behavior of **5** in solution, a pendulum-like exchange of the positions of Zn1 and Zn2 atoms was proposed (Fig. 5). This "pendulum" mechanism assumes an inversion at the imino nitrogen N3 as well as the decoordination/recoordination of Zn1 from N5 to N3 and of Zn2 from N3 to N4. The inversion on both methoxy groups should be taken into the account as well. As shown by the solid-state structure of the complex **5**, the unique placement of the two Dipp groups at the base of the ligand unlocks the system and enables this movement. For this sequence of structural changes, we have found two different transition states (Fig. 5, mol and gif files in SI) whose energy exceeds that of the optimized structure of **5** by 40.36 and 22.83 kcal/mol, respectively.

ROP Catalysis

All the monometallic and bimetallic zinc complexes prepared were investigated as catalysts for the ROP of *rac*-LA (reduced Table 1 and full Table S2). The complexes **2** and **3** showed no activity after 2 hours at 25 °C in CH_2Cl_2, even in the presence of one eq. of ^{i}PrOH as a co-initiator. The bis(trimethylsilylamido) complexes **4** and **5** exhibited modest activities, reaching monomer conversion of 61% and 32% in 2 hours at 25 °C without ^{i}PrOH (Table 1, entries 1 and 2). Remarkably, the GPC analysis of the PLA chains thus formed showed much higher average molecular weights than the theoretical M_n values calculated on the bases of LA conversion and LA:Cat ratio. These results suggest a slower initiation than propagation. Unlike in the complexes **2** and **3**, the use of ^{i}PrOH as a co-initiator

in the complexes **4** and **5** greatly improved their performance. In the presence of one eq. alcohol per Zn metal center, both complexes, initiated the ROP of 100 equiv. *rac*-LA with almost complete conversion in 1 min and led to slightly heterotactic PLA with narrow dispersity and good agreement between theoretical and experimental M_n values, albeit with slightly higher molar mass than expected in the case of **5** (Table 1, entries 3 and 4). It is noteworthy that an increase in the **5**:^{i}PrOH ratio to 1:1 (0.5 eq. of alcohol per Zn) decreased monomer conversion, highlighting the poor ability of the residual amido group on Zn to initiate the polymerization (entry 5).

At lower catalyst loading (0.2 mol% equiv. of Zn), the bimetallic complex **5** lags behind the complex **4**, giving 86% conversion in 15 minutes, whereas the complex **4** has achieved full conversion in 5 minutes (Table S2, entries 9–10). At 0.1-mol% catalytic loading, the complex **4** has enabled complete monomer conversion in 5 min and 83% conversion in 3 min, ranking it as the most active monometallic Zn catalyst for LA ROP (TOF = 16,600 h^{-1}) (Table 1, entry 7). Here, narrowly dispersed PLA chains with the molar masses of 116,200 and 110,700 $g.mol^{-1}$ have been obtained. Although high, these values are slightly lower than the theoretical ones, probably due to the presence of residual water in the CH_2Cl_2 or lactide. The complexes **4** and **5** were subsequently tested under chain-transfer conditions, in the presence of 10 equiv. of alcohol and at the catalytic loading of 0.02 mol% (equiv. of Zn) (Table 1, entries 8–9). Under these conditions, the best performance was exhibited by the bimetallic complex **5**, yielding a narrow-disperse PLA with predictable M_n and 90% monomer conversion in 20 minutes (TOF = 13,500 h^{-1}), 10 minutes less than its monometallic counterpart. With the aim of obtaining more information on the ROP mechanism with the complexes **4** and **5**, PLA chain-end group analysis, alcoholysis experiments on the complexes and kinetic studies were carried out. The MALDI-TOF MS spectrometric analysis of PLA samples produced either from **4** or **5** with ^{i}PrOH in a 1:1 ratio and 25 molar equiv. of LA (100% conversion, 1 min) showed in both cases isopropoxy-terminated chains with a peak spacing of 144 Da and some minor intercalated peaks due to transesterification reactions (see SI, Fig. S38–S40). A kinetic study carried out with the complexes **4** and **5** in CH_2Cl_2 at room temperature tends to confirm this hypothesis. The semilogarithmic plot of *rac*-LA with time shows linear relationship at different concentrations of the complex **4**, indicating a first-order kinetic in monomer concentration (Fig. 6a). The evolution of the M_n and Đ values with conversion confirmed the well-controlled character of the polymerization. The slopes of the fitted lines of log k_{app} *vs* log[**4**] and k_{app} *vs* [**4**] indicate a first order in catalyst concentration and the rate constant k_p of 386 $M^{-1}.min^{-1}$, which is higher than those reported for the best monometallic Zn complexes described to date (Fig. 6b and Fig. S37a, S37c). Polymerization with the bimetallic complex **5** proceeds with first-order dependence in monomer when using one equivalent of ^{i}PrOH (0.5 mol. equiv. per Zn) and with second-order dependence in monomer when using one equiv. of co-initiator per Zn metal center (Fig. 6c–d and Fig. S37b). In the latter case, the dependence of ln k_{app} *vs* ln [**5**] was analyzed; it indicates a first order in the bimetallic complex **5,** giving a global kinetic law of the form: $-d[LA]/dt = k_p[\mathbf{5}]^1[LA]^2$. The first-order dependence on **5** and the second-order dependence on lactide strongly imply that the integrity of the bimetallic biguanide–Zn complex is preserved under catalytic conditions.[44]

We have attempted to prepare, isolate and structurally characterize alkoxy-zinc biguanides, presumed to be the species responsible for the performance of the process. To generalize the results, the alcoholysis of all the complexes yields mixed oligomers of $\{[(Me_3Si)_2N]Zn\text{-}\mu^2\text{-}O^iPr\}_2$ or $[EtZn\text{-}\mu^3\text{-}O^iPr]_4$ along with **1** and **6** (the homoleptic zinc complex – for details, see SI, pp. S32–S36).

As the homoleptic complex **6** is suspected to form under catalytic conditions, we performed the ROP of *rac*-LA in the presence of **6**. The results showed that it was active, but much less than **4** and **5**, producing PLA with only 10% conversion after 1 minute at room temperature and with 1-mol% catalyst loading (Table S2, entry 15). It should be highlighted that the combination of $Zn[N(SiMe_3)_2]_2$ and alcohol has been previously described as an effective catalyst for the ROP of cyclic esters. Therefore, we performed ROP tests using $Zn[N(SiMe_3)_2]_2$/^{i}PrOH (1:1), biguanide/^{i}PrOH (1:1) or a mixture of biguanide, $Zn[N(SiMe_3)_2]_2$ and ^{i}PrOH in a 1:1:1 ratio (Table S2, entries 16–18). All these combinations failed to match the performance of complexes **4** and **5**, both in terms of activity and polymerization control, indicating that the biguanide–Zn and Zn–biguanide–Zn entities are preserved under catalytic conditions and responsible for the catalytic activity.

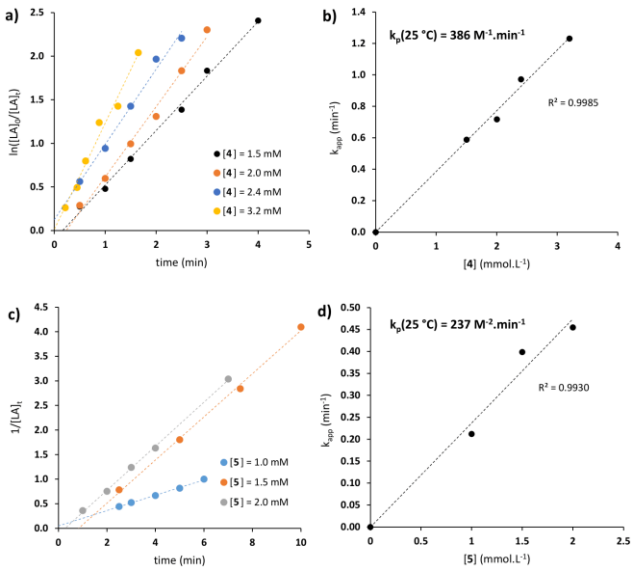

Figure 6. a) A first-order semi-logarithmic plot for the polymerization of *rac*-LA at 25°C in CH_2Cl_2 using **4** at different concentrations with ^{i}PrOH as a co-initiator. b) A plot of k_{app} *vs* $[\mathbf{4}]_0$. c) A second-order plot for the polymerization of *rac*-LA at 25 °C in CH_2Cl_2 using **5** at different concentrations with ^{i}PrOH as a co-initiator. d) A plot of k_{app} *vs* $[\mathbf{5}]_0$.

The complexes **4** and **5** were also tested for the ROP of the more reluctant *rac*-*β*-butyrolactone (BL) monomer (see Table 2). Under optimized conditions, the complexes **4** and **5** exhibited moderate activity toward the ROP of BL, affording narrow-disperse PHB with 94% and 63% conversion, respectively, after 3 hours at 45°C in CH_2Cl_2 at 1 mol% catalyst loading.

To the best of our knowledge, a di- or triblock copolymers from *L*-lactide, *D*-lactide and *rac*-lactide prepared by a sequential addition of monomers to the solution of primary polymer with homoleptic zinc complex bearing chelating amino-phenoxy ligand were reported only very recently.[19] Lactide copolymerization with β-butyrolactone feasible *via* irreversible process driven sequentially by discrete combination of Zn and Y complexes was published by Robinson[9] during the completing of this work. Our successful result of β-butyrolactone and lactide polymerization led us to the idea to investigate one-pot synthesis of diblock copolymers (PHB-*co*-PLLA) with the complex **4** by sequential addition of the two monomers. The addition of butyrolactone first, followed by *L*-lactide, proved more efficient than the reverse, leading to the diblock copolymer with BL and LA conversions of 90% after a sequence at 45 °C for 3 hours for the ROP of BL and 1 min at 20 °C

for LA. The GPC analysis of the copolymer chains thus formed showed a unimodal distribution, a narrow Đ and the average molecular-weight number consistent with that calculated on the basis of the ratio of monomers and conversions (Fig. S36). DOSY (diffusion ordered spectroscopy) NMR analysis revealed a unique diffusion coefficient of 1.22 x10^{-10} $m^2.s^{-1}$ ($CDCl_3$, 298 K), also consistent with the formation of copolymer chains rather than a mixture of homopolymers (Fig. 7).

The average molecular weight close to that found by GPC analysis could be determined on the basis of DOSY calibration experiments ($M_{n,\,DOSY}$ = 10,300 g.mol) (see SI, Table S4 and Fig. S33). No trace resonances attributed to the PLA-PHB linking units were detected in ^{1}H NMR, that would attest the formation of only a diblock (PHB-*co*-PLA) without secondary transesterification reactions (Fig. S32 in SI). The living nature of the polymerization was further confirmed by the addition of a third batch of 50 equiv. of *D*-LA, resulting in a PHB-*co*-PLLA-*co*-PDLA triblock *at*-sb-*st*-sb-*st* copolymer

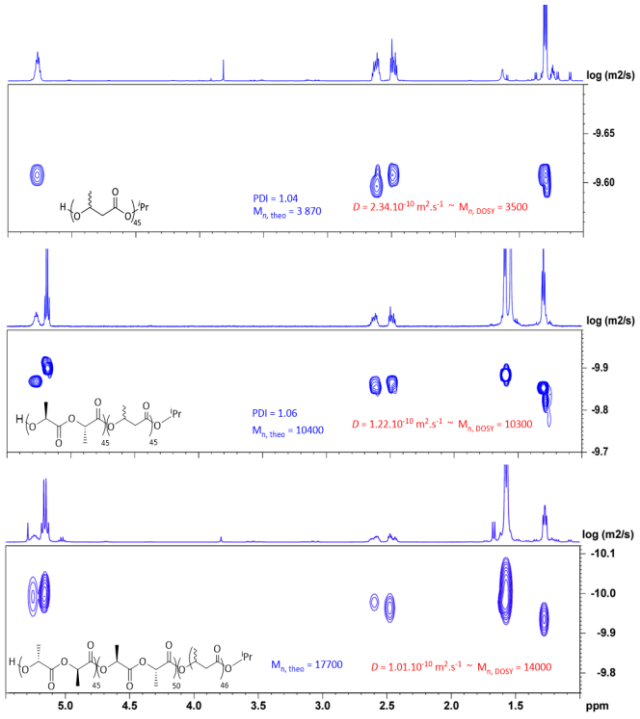

Figure 7. The DOSY NMR spectra of PHB (upper panel), PLLA-*co*-PHB (middle panel, Table 2, entry 5) and PDLA-*co*-PLLA-*co*-PHB (lower panel – Table 2, entry 7) in $CDCl_3$.

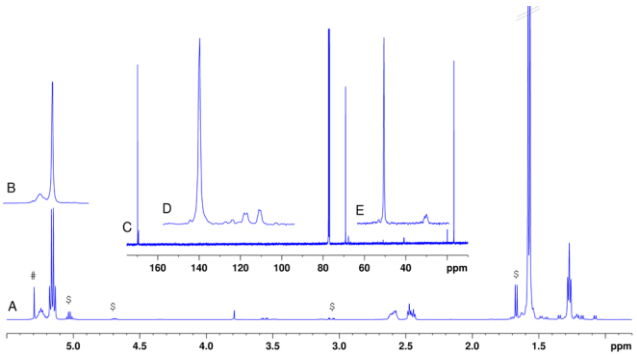

Figure 8. ^{1}H (A), 1D-^{1}H selective decoupled (B) and ^{13}C NMR spectra (C) with details of the carbonyl (D) and methine regions (E) of a crude mixture of PHB-*co*-PLLA-*co*-PDLA, Table 2, entry 7) in $CDCl_3$. Unreacted monomers ($) and CH_2Cl_2 (#) are marked.

(Table 2, entry 6). The triblock copolymer was insoluble in THF, precluding GPC measurements in this solvent. Nevertheless, DOSY NMR analysis confirmed the formation of a unique triblock copolymer with a diffusion coefficient equal to 1.01 x 10^{-10} $m^2.s^{-1}$ ($CDCl_3$, 298 K) and the estimated M_n value of 14 000 based on PLA-curve calibration (Fig. 7 – lower panel). The ^{1}H NMR spectrum of the triblock copolymer shows a single quartet attributed to the methine (CH) signal of the two PLA stereoblocks, indicating that transesterification or *L*/*D* LA monomer scrambling events are minimal (Fig. 8). In addition, we were able to prepare a triblock copolymer with PHB as the middle block. The incorporation of an atactic PLA chain instead of isotactic PLLA as the initial block did not impede the ROP of BL to the same extent as observed in the synthesis of PLLA-*co*-PHB diblocks (Table 2, entries 7 and 4). GPC data show a unimodal profile with the M_n value slightly lower than predicted and narrow dispersity (Đ = 1.26). At last, the dinuclear complex **5** was also shown to be able to promote the formation of the PLA-*co*-PHB-*co*-PLA triblock, although longer reaction times were required to build the last two PHB and PLA blocks. All these results showed the ability of both complexes **4** and **5** to promote the synthesis of diblock and/or triblock copolymers in a controlled and living manner.

Conclusions

Mono- and dizinc complexes with the cheap, easily accessible and structurally versatile ditopic biguanide proligand **1** were synthesized by one-step protocol. While the ethylzinc complexes **2** and **3** are inactive in the ROP of *rac*-lactide, the performance of the zinc amides **4** and **5** is striking after their activation by ^{i}PrOH: *i)* the highest TOF number 16,600 h^{-1} for **4** and 13,500 h^{-1} for **5**; *ii)* very high M_n under mild polymerization conditions (the highest value of 116,200 g.mol^{-1} for **4** and 67,100 g.mol^{-1} for **5**; *iii)* narrow polydispersity values. Based on the most independent, comparable and valuable criterion, the rate constant k_p, their catalytic performance, (k_p(25 °C) of 386 M^{-1}.min^{-1} for **4** and 237 M^{-2}.min^{-1} for **5**), exceeding the highest value reported by Robinson[4] (~300 M^{-1}.min^{-1}, Fig. S37c, SI). These observations assign **4** and **5** the role of some of the most efficient catalysts when the lactide ROP is activated by ^{i}PrOH. Because of the structurally versatile behavior of the biguanide ligand, the complex **5** undergoes a possible mutual interchange of the positions of zinc atoms, which is in contrast to the monometallic **4** or the bimetallic **3** with the Zn atom position locked to the "BDI" side. This could explain the ability of this "dissymmetric" bimetallic complex to promote the ROP of LA at both Zn sites, either at the same time or consecutively, to form PLA chains with a unimodal molecular-weight distribution. In order to get closer industrial conditions, we preliminary tested thermal robustness of **5** in boiling toluene as well as in the solid state at 160°C and the catalytic performance of it in polymerization of recrystallized technical grade *rac*-lactide exhibiting promising results, which This will be a subject of our further studies.

Successful consecutive living copolymerization of *β*-butyrolactone with either *L*-, *D*- or *rac*-lactide giving di- and triblock copolymers with narrow dispersity opens the door to the preparation of various di- or oligoblock heterocopolymers. Most surprisingly, these processes are performed with only one portion of the zinc complex and alcohol; after the completion of each step, it is only necessary to change monomers and temperature. In comparison with the recent literature,[9] in order to achieve a similar copolymer (but only diblock), it is necessary to add two different catalysts with different metals and ligands plus monomers in a batch process at elevated temperature.

ASSOCIATED CONTENT

Supporting Information. Synthetic procedures, the explanation of proligand equilibria, alcoholysis, the dynamic behavior of **5**, crystal-structure parameters, cif & mol files.

AUTHOR INFORMATION

Corresponding Authors

*tomas.chlupaty@upce.cz (Tomáš Chlupatý), pierre.le-gendre@u-bourgogne.fr (Pierre Le Gendre) and ales.ruzicka@upce.cz (Aleš Růžička).

Author Contributions

The manuscript was written through contributions of all authors. All authors have given approval to the final version of the manuscript. [a]B. T. and L. V. contributed equally. Benjamin Théron: investigation, ROP catalysis; Lukáš Vlk: investigation, synthesis, ROP catalysis, writing; Tomáš Chlupatý: investigation, synthesis, catalysis, NMR spectroscopy, writing; Eliška Procházková: VT NMR, writing; Marie-José Penouilh: DOSY NMR; Raluca Malacea-Kabbara: conceptualization, supervision, writing; Pierre Le Gendre: conceptualization, supervision, writing; Aleš Růžička: conceptualization, supervision, X-ray diffraction analysis, calculations, writing.

ACKNOWLEDGMENT

This work was supported by the Czech Science Foundation grant no. 21-02964S. Research infrastructure project CZ.02.01.01/00/23_021/0008593 (Innovative materials suitable for high added value applications (INMA)) and a bilateral Czech-French project PHC BARRANDE 2024 50539QG are acknowledged.

REFERENCES

1. Haider, T. P.; Völker, C.; Kramm, J.; Landfester, K.; Wurm, F. R. Plastics of the Future? The Impact of Biodegradable Polymers on the Environment and on Society. *Angew. Chem. Int. Ed.* **2019,** *58*, 50–62.

2. Dana, H. R.; Ebrahimi, F. Synthesis, properties, and applications of polylactic acid-based polymers. *Polym. Eng. Sci*. **2023**, *63*, 22-43.

3. Cheng, M.; Attygalle, A. B.; Lobkovsky, E. B.; Coates, G. W. Single-Site Catalysts for Ring-Opening Polymerization: Synthesis of Heterotactic Poly(lactic acid) from *rac*-Lactide. *J. Am. Chem. Soc*. **1999**, *121*, 11583–11584.

4. Chellali, J. E.; Alverson, A. K.; Robinson, J. R. Zinc Aryl/Alkyl *β*-diketiminates: Balancing Accessibility and Stability for High-Activity Ring-Opening Polymerization of *rac*-Lactide. *ACS Catal*. **2022**, *12*, 5585–5594.

5. Thevenon, A.; Romain, C.; Bennington, M. S.; White, A. J. P.; Davidson, H. J.; Brooker, S.; Williams, C. K. Dizinc Lactide Polymerization Catalysts: Hyperactivity by Control of Ligand Conformation and Metallic Cooperativity. *Angew. Chem*. **2016**, *55*, 8680–8685.

6. Coles, M. P.; Hitchcock, P. B. Zinc Guanidinate Complexes and Their Application in Ring-Opening Polymerisation Catalysis. *Eur. J. Inorg. Chem.* **2004**, *2004*, 2662–2672.

7. D'Auria, I.; Ferrara, V.; Tedesco, C.; Kretschmer, W.; Kempe, R.; Pellecchia, C. Guanidinate Zn(II) Complexes as Efficient Catalysts for Lactide Homo- and Copolymerization under Industrially Relevant Conditions. *ACS Appl. Polym. Mater*. **2021**, *3*, 4035–4043.

8. Sou, H.; Liu, S.; Liu, J.; Zhang, Z.; Qu, R.; Gu, Y.; Qin, Y. Novel epoxide-promoted polymerization of lactides mediated by a zinc guanidine complex: a potential strategy for the tin-free PLA industry. *Polym. Chem.* **2023**, *14*, 4652–4658.

9. Chellali, J. E.; Woodside, A. J.; Yu, Z.; Neogi, S.; Külaots, I.; Guduru, P. R.; Robinson, J. R. Access to Stereoblock Polyesters *via* Irreversible Chain-Transfer Ring-Opening Polymerization (ICT-ROP). *J. Am. Chem. Soc.* **2024**, *146*, 11562−11569.

10. Diaz, C.; Mehrkhodavandi, P. Strategies for the synthesis of block copolymers with biodegradable polyester segments *Polym. Chem.* **2021**, *12*, 783–806.

11. Aluthge, D. C.; Xu, C.; Othman, N.; Noroozi, N.; Hatzikiriakos, S. G.; Mehrkhodavandi, P. PLA–PHB–PLA Triblock Copolymers: Synthesis by Sequential Addition and Investigation of Mechanical and Rheological Properties. *Macromolecules* **2013**, *46*, 3965−3974.

12. Xu, C.; Yu, I.; Mehrkhodavandi, P. Highly controlled immortal polymerization of β-butyrolactone by a dinuclear indium catalyst. *Chem. Commun.* **2012**, *48*, 6806–6808.

13. Yu, I.; Ebrahimi, T.; Hatzikiriakos, S. G.; Mehrkhodavandi, P. Star-shaped PHB–PLA block copolymers: immortal polymerization with dinuclear indium catalysts. *Dalton Trans*. **2015**, *44*, 14248–14254.

14. Ebrahimi, T.; Aluthge, D. C.; Patrick, B. O.; Hatzikiriakos, S. G.; Mehrkhodavandi, P. Air- and Moisture-Stable Indium Salan Catalysts for Living Multiblock PLA Formation in Air. *ACS Catal.* **2017**, *7*, 6413–6418.

15. Rosen, T.; Goldberg, I.; Navarra, W.; Venditto, V.; Kol, M. Divergent [{ONNN}Mg–Cl] complexes in highly active and living lactide polymerization. *Chem. Sci.* **2017**, *8*, 5476–5481.

16. Sanchez, L. A. H.; Woroch, C. P.; Dumas, D. M.; Waymouth, R. M.; Kanan, M. W. Toughening Poly(lactic acid) without Compromise – Statistical Copolymerization with a Bioderived Bicyclic Lactone. *J. Am. Chem. Soc.* **2025**, *147*, 5212−5219.

17. Rosen, T.; Goldberg, I.; Venditto, V.; Kol, M. Tailor-Made Stereoblock Copolymers of Poly(lactic acid) by a Truly Living Polymerization Catalyst. *J. Am. Chem. Soc.* **2016**, *138*, 12041–12044.

18. D'Auria, I.; D'Alterio, M. C.; Tedesco, C.; Pellecchia, C. Tailor-made block copolymers of L-, D- and rac-lactides and ε-caprolactone via one-pot sequential ring opening polymerization by pyridylamidozinc(II) catalysts. *RSC Adv.* **2019**, *9*, 32771–32779.

19. Pongpanit, T.; Saeteaw, T.; Chumsaeng, P.; Chasing, P.; Phomphrai, K. Highly Active Homoleptic Zinc and Magnesium Complexes Supported by Constrained Reduced Schiff Base Ligands for the Ring-Opening Polymerization of Lactide. *Inorg. Chem*. **2021**, *60*, 17114−17122.

20. Chisholm, M. H.; Gallucci, J. C.; Phomphrai, K. Comparative Study of the Coordination Chemistry and Lactide Polymerization of Alkoxide and Amide Complexes of Zinc and Magnesium with a β-Diiminato Ligand Bearing Ether Substituents. *Inorg. Chem.* **2005**, *44*, 8004–8010.

21. Kernbichl, S.; Reiter, M.; Mock, J.; Rieger, B. Terpolymerization of β-Butyrolactone, Epoxides, and CO_2: Chemoselective CO_2-Switch and Its Impact on Kinetics and Material Properties. *Macromolecules* **2019**, *52*, 8476–8483.

22. Fagerland, J.; Finne-Wistrand, A.; Pappalardo, D. Modulating the thermal properties of poly(hydroxybutyrate) by the copolymerization of *rac*-β-butyrolactone with lactide. *New J. Chem.* **2016**, *40*, 7671–7679.

23. García-Valle, F. M.; Tabernero, V.; Cuenca, T.; Mosquera, M. E. G.; Cano, J.; Milione, S. Biodegradable PHB from *rac*-β-Butyrolactone: Highly Controlled ROP Mediated by a Pentacoordinated Aluminum Complex. *Organometallics* **2018**, *37*, 837–840.

24. García-Valle, F. M.; Cuenca, T.; Mosquera, M. E. G.; Milione, S.; Cano, J. Ring-Opening Polymerization (ROP) of cyclic esters by a versatile aluminum Diphenoxyimine Complex: From polylactide to random copolymers. *Eur. Pol. J.* **2020**, *125*, 109527–109535.

25. Zheng, X.-X.; Wang, Z.-X. Synthesis of aluminum complexes supported by 2-(1,10-phenanthrolin-2-yl)phenolate ligands and their catalysis in the ring-opening polymerization of cyclic esters. *RSC Adv.* **2017**, *7*, 27177–27188.

26. Platel, R. H.; Hurst, A. R. Precise Microstructure Control in Poly(hydroxybutyrate-*co*-lactic Acid) Copolymers Prepared by an Yttrium Amine Bis(phenolate) Complex. *Macromolecules* **2020**, *53*, 10773–10784.

27. Jeffery, B. J.; Whitelaw, E. L.; Garcia-Vivo, D.; Stewart, J. A.; Mahon, M. F.; Davidson, M. G.; Jones, M. D. Group 4 initiators for the stereoselective ROP of *rac*-β-butyrolactone and its copolymerization with *rac*-lactide. *Chem. Commun.* **2011**, *47*, 12328–12330.

28. Whitehorne, T. J. J.; Schaper, F. Lactide, β-butyrolactone, δ-valerolactone, and ε-caprolactone polymerization with copper diketiminate complexes. *Can. J. Chem.* **2014**, *92*, 206–214.

29. Chlupatý, T.; Nevoralová, J.; Růžičková, Z.; Růžička, A. Lithium and Dilithium Guanidinates, a Starter Kit for Metal Complexes Containing Various Mono- and Dianionic Ligands. *Inorg. Chem.* **2020**, *59*, 10854–10865.

30. Bailey, C. J. Metformin: historical overview. *Diabetologia*. **2017**, *60*, 1566–1576.

31. Viollet, B.; Guigas, B.; Garcia, N. S.; Leclerc, J.; Foretz, M.; Andreelli, F. Cellular and molecular mechanisms of metformin: an overview. *Clin. Sci*. **2012**, *122*, 253–270.

32. Foretz, M.; Guigas, B.; Bertrand, L.; Pollak, M.; Viollet, B. Metformin: From Mechanisms of Action to Therapies. *Cell Metab*. **2014**, *20*, 953–966.

33. Kathuria, D.; Raul, A. D.; Wanjari, P.; Bharatam, P. V. Biguanides: Species with versatile therapeutic applications. *Eur. J. Med. Chem*. **2021**, *219*, 113378–113416.

34. Peddarao, T.; Sarkar, N.; Nembenna, S. Mono- and Bimetallic Aluminum Alkyl, Alkoxide, Halide and Hydride Complexes of a Bulky Conjugated Bis-Guanidinate(CBG) Ligand and Aluminum Alkyls as Precatalysts for Carbonyl Hydroboration. *Inorg. Chem.* **2020**, *59*, 4693–4702.

35. Sahoo, R. K.; Sarkar, N.; Nembenna, S. Zinc Hydride Catalyzed Chemoselective Hydroboration of Isocyanates: Amide Bond Formation and C=O Bond Cleavage. *Angew. Chem. Int. Ed*. **2021**, *60*, 11991–12000.

36. Peddarao, T.; Baishya, A.; Sarkar, N.; Acharya, R.; Nembenna, S. Conjugated Bis-Guanidines (CBGs) as *β*-Diketimine Analogues: Synthesis, Characterization of CBGs/Their Lithium Salts and CBG Li Catalyzed Addition of B−H and TMSCN to Carbonyls. *Eur. J. Inorg. Chem.* **2021**, *2021*, 2034–2046.

37. Sahoo, R. K.; Mahato, M.; Jana, A.; Nembenna, S. Zinc Hydride Catalyzed Hydrofuntionalization of Ketones. *J. Org. Chem*. **2020**, 85, 11200–11210.

38. Glöckler, E.; Ghosh, S.; Schulz, S. *β*-Diketiminate and *β*-Ketoiminate Metal Catalysts for Ring-Opening Polymerization of Cyclic Esters. *Polym. Rev.* **2022**, *63*, 478–514.

39. Webster, R. L. *β*-Diketiminate complexes of the first row transition metals: applications in catalysis. *Dalton Trans*. **2017**, *46*, 4483–4498.

40. Sarish, S. P.; Nembenna, S.; Nagendran, S.; Roesky, H. W. Chemistry of Soluble β-Diketiminatoalkaline-Earth Metal Complexes with M−X Bonds (M = Mg, Ca, Sr; X = OH, Halides, H). *Acc. Chem. Res*. **2017**, *44*, 157–170.

41. Bourget-Merle, L.; Lappert, M. F.; Severn, J. R. The Chemistry of *β*-Diketiminatometal Complexes. *Chem. Rev.* **2002**, *102*, 3031–3066.

42. Thakur, M.; Singh, N.; Sharma, A.; Rana, R.; Abdul Syukor, A. R.; Naushad, M.; Kumar, S.; Singh, L. Metal coordinated macrocyclic complexes in different chemical transformations. *Coord. Chem. Rev*. **2022**, *471*, 214739.

43. Tian, D.; Xie, Q.; Yan, L.; Tong, H.; Zhou, M. Zinc and aluminum complexes derived from 2,4-*N*,*N*′-disubstituted 1,3,5-triazapentadienyl ligands: Synthesis, characterization and catalysis of the ring-opening polymerization of *rac*-lactide. *Inorg. Chem. Commun*. **2015**, *58*, 35–38.

44. Wu, J.-C.; Huang, B.-H.; Hsueh, M.-L.; Lai, S.-L.; Lin, C.-C. Ring-opening polymerization of lactide initiated by magnesium and zinc alkoxides. *Polymer* **2005**, *46*, 9784-9792.

Graphical Abstract / Synopsis

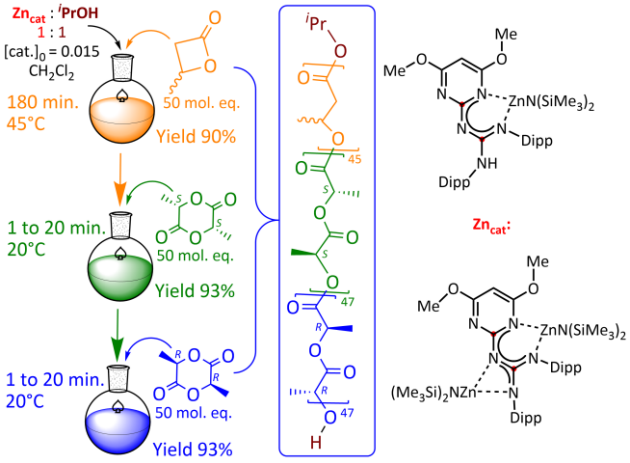
Zncat : iPrOH
1 : 1
[cat.]0 = 0.015
CH2Cl2
180 min.
45°C
50 mol. eq.
Yield 90%
1 to 20 min.
20°C
50 mol. eq.
Yield 93%
1 to 20 min.
20°C
50 mol. eq.
Yield 93%
iPr
45
47
47
H
Me
Me
ZnN(SiMe3)2
Dipp
NH
Dipp
Zncat:
Me
Me
ZnN(SiMe3)2
Dipp
(Me3Si)2NZn
Dipp